Article

Residue Ionization in LpxC Directly Observed by Zn NMR Spectroscopy

Andrew S. Lipton, Robert W. Heck, Marcy Hernick, Carol A. Fierke, and Paul D. Ellis

J. Am. Chem. Soc., **2008**, 130 (38), 12671-12679 • DOI: 10.1021/ja801776c • Publication Date (Web): 30 August 2008

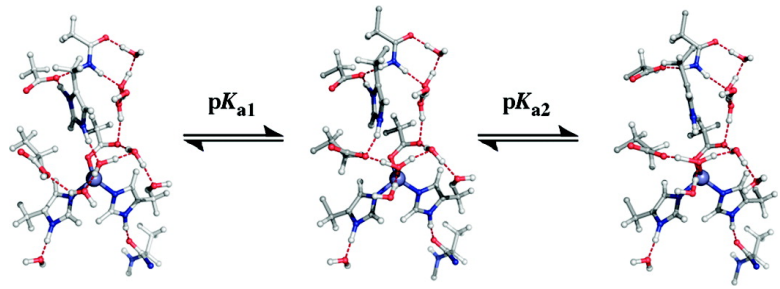

J|A|C|S
ARTICLES

Published on Web 08/30/2008

Residue Ionization in LpxC Directly Observed by ^{67}Zn NMR Spectroscopy

Andrew S. Lipton,[†] Robert W. Heck,[†] Marcy Hernick,[‡,§] Carol A. Fierke,*[,‡] and Paul D. Ellis*[,†]

Biological Sciences Division, Pacific Northwest National Laboratory, 902 Battelle Boulevard, Richland, Washington 99352, and Department of Chemistry, University of Michigan, 930 North University, Ann Arbor, Michigan 48109

Received March 12, 2008; E-mail: fierke@umich.edu; paul.ellis@pnl.gov

Abstract: The pH dependence of the solid-state ^{67}Zn NMR lineshapes has been measured for both the wild type (WT) and the H265A mutant of *Aquifex aeolicus* LpxC, each in the absence of substrate (resting state). The ^{67}Zn NMR spectrum of WT LpxC at pH 6 (prepared at 0 °C) contains two overlapping quadrupole lineshapes with C_q values of 10 and 12.9 MHz, while the spectrum measured for the sample prepared at a pH near 9 (at 0 °C) is dominated by the appearance of a third species with a C_q of 14.3 MHz. These findings are consistent with the two pK_a values previously observed by the bell-shaped dependence of the LpxC-catalyzed reaction. On the basis of comparison of the experimental results with predictions from quantum mechanical/molecular mechanical (QM/MM) modeling, we suggest that pK_{a1} (low pH) represents the ionization of Glu78 and pK_{a2} (high pH) reflects the ionization of another active site residue located near the zinc ion, such as His265. These results are also consistent with water being bound to the Zn^{2+} ion throughout this pH range. The ^{67}Zn NMR spectra of the H265A mutant appear to be pH independent, with a C_q of 9.55 MHz being sufficient to describe both low- and high-pH data. The QM/MM models of the H265A mutant suggest that over this pH range water is bound to the zinc ion while Glu78 is protonated.

Introduction

Lipid A is the hydrophobic anchor of lipopolysaccharides (LPSs) that make up the outer membrane of Gram-negative bacteria and is the component of LPSs responsible for bacterial sepsis and septic shock.[1,2] LpxC is a metal-dependent deacetylase that uses a single divalent metal ion to catalyze the committed step in the biosynthesis of lipid A, the hydrolysis of UDP-3-*O*-myristoyl-*N*-acetyl-glucosamine to form UDP-3-*O*-myristoyl-glucosamine and acetate.[1] Lipid A is essential for the survival of Gram-negative bacteria, as the loss of lipid A results in decreased viability and increased sensitivity to antibiotics; consequently, inhibitors of lipid A biosynthesis have the potential to serve both as antimicrobial agents and, in the case of septic shock, as antiendotoxins.[2] Inhibitors of the bacterial enzyme LpxC have demonstrated antibacterial activity against a wide range of Gram-negative organisms, including those associated with cystic fibrosis (*Pseudomonas aeruginosa*, *Burkholderia cepacia*, and *Haemophilus influenzae*),[3−8] thus validating LpxC as an antimicrobial target. The three-dimensional structure of LpxC from *Aquifex aeolicus* has been solved, revealing a novel $\alpha + \beta$ fold with a His_2Asp zinc binding motif[9−12] similar to that of Zn_1 in alkaline phosphatase.[13−15] Neither the three-dimensional structure nor the sequence of LpxC shows significant homology with other metalloamidases, suggesting the potential for novel mechanistic features. Mu-

[†] Pacific Northwest National Laboratory.
[‡] University of Michigan.
[§] Current address: Department of Biochemistry, Virginia Tech, Engel Hall, Blacksburg, VA 24061.

(1) Jackman, J. E.; Raetz, C. R. H.; Fierke, C. A. *Biochemistry* **1999**, *38*, 1902–1911.
(2) Wyckoff, T. J. O.; Raetz, C. R. H.; Jackman, J. E. *Trends Microbiol.* **1998**, *6*, 154–159.
(3) Onishi, H. R.; Pelak, B. A.; Gerckens, L. S.; Silver, L. L.; Kahan, F. M.; Chen, M. H.; Patchett, A. A.; Galloway, S. M.; Hyland, S. A.; Anderson, M. S.; Raetz, C. R. H. *Science* **1996**, *274*, 980–982.
(4) Jackman, J. E.; Fierke, C. A.; Tumey, L. N.; Pirrung, M.; Uchiyama, T.; Tahir, S. H.; Hindsgaul, O.; Raetz, C. R. H. *J. Biol. Chem.* **2000**, *275*, 11002–11009.
(5) Pirrung, M. C.; Tumey, L. N.; Raetz, C. R. H.; Jackman, J. E.; Snehalatha, K.; McClerren, A. L.; Fierke, C. A.; Gantt, S. L.; Rusche, K. M. *J. Med. Chem.* **2002**, *45*, 4359–4370.
(6) Clements, J. M.; Coignard, F.; Johnson, I.; Chandler, S.; Palan, S.; Waller, A.; Wijkmans, J.; Hunter, M. G. *Antimicrob. Agents Chemother.* **2002**, *46*, 1793–1799.
(7) Kline, T.; et al. *J. Med. Chem.* **2002**, *45*, 3112–3129.
(8) White, R. J.; Margolis, P. S.; Trias, J.; Yuan, Z. Y. *Curr. Opin. Pharmacol.* **2003**, *3*, 502–507.
(9) Whittington, D. A.; Rusche, K. M.; Shin, H.; Fierke, C. A.; Christianson, D. W. *Proc. Natl. Acad. Sci. U.S.A.* **2003**, *100*, 8146–8150.
(10) Coggins, B. E.; Li, X. C.; McClerren, A. L.; Hindsgaul, O.; Raetz, C. R. H.; Zhou, P. *Nat. Struct. Biol.* **2003**, *10*, 645–651.
(11) Hernick, M.; Gennadios, H. A.; Whittington, D. A.; Rusche, K. M.; Christianson, D. W.; Fierke, C. A. *J. Biol. Chem.* **2005**, *280*, 16969–16978.
(12) Coggins, B. E.; McClerren, A. L.; Jiang, L.; Li, X.; Rudolph, J.; Hindsgaul, O.; Raetz, C. R. H.; Zhou, P. *Biochemistry* **2005**, *44*, 1114–1126.
(13) Sowadski, J. M.; Handschumacher, M. D.; Murthy, H. M.; Foster, B. A.; Wyckoff, H. W. *J. Mol. Biol.* **1985**, *186*, 417–33.
(14) Sowadski, J. M.; Handschumacher, M. D.; Murthy, H. M.; Kundrot, C. E.; Wyckoff, H. W. *J. Mol. Biol.* **1983**, *170*, 575–81.
(15) Sowadski, J. M.; Foster, B. A.; Wyckoff, H. W. *J. Mol. Biol.* **1981**, *150*, 245–72.

Scheme 1

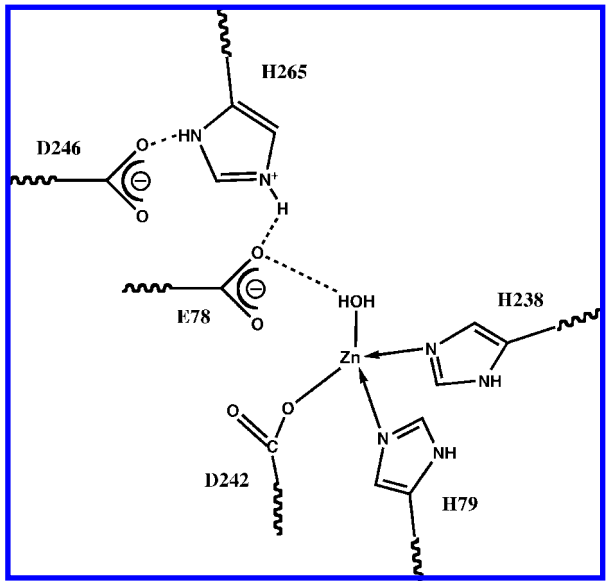

tagenesis and structural studies suggest that LpxC functions via a general-acid−base-catalyst pair mechanism using the side chains of Glu78[16] (GBC) and His265 (GAC) rather than the canonical single general-acid−base-catalyzed mechanism proposed for most metalloproteases.[11,17] The zinc−water complex is the proposed nucleophile in the reaction, while the catalytic zinc ion is proposed to function by lowering the pK_a of the metal-bound water and providing electrostatic stabilization of the transition states throughout the course of the reaction.[11]

Scheme 1 shows a representation of the residues that have been implicated to participate in the reaction mechanism for LpxC (using the *Escherichia coli* numbering). This scheme depicts the protonation state of the resting enzyme at neutral pH on the basis of structural[9] and biochemical[11,18] studies where the mechanism for LpxC is proposed to involve a doubly protonated His265 residue functioning as either a general acid or an electrostatic catalyst and the side chain of Glu78 acting as a general base in the reaction. Mutagenesis experiments have identified side chains that are important for catalytic activity, including Glu78, Thr191, Lys239, Asp246, and His265.[7,9−11] The H265A mutation in *A. aeolicus* (*Aa*) LpxC reduces catalytic activity (k_{cat}/K_M) by ~170-fold, while the E78A/H265A double mutation further decreases activity by an additional order of magnitude (1700-fold reduced).[11] The LpxC-catalyzed reaction exhibits a bell-shaped dependence on pH with two apparent pK_a values of 5.8 and 7.9 for the wild-type (WT) *Aa* LpxC at 60 °C (the values shift to 6.2 and 9.2 for the *E. coli* (*Ec*) enzyme at 30 °C).[11,18] Results from mutagenesis experiments suggest that the pK_{a1} value observed in activity measurements reflects ionization of Glu78.[11,18] On the basis of its value, pK_{a2} has been proposed to reflect ionization of His265 or the zinc−water complex. The value of pK_{a2} varies with the identity of the active site metal ion (Zn, Ni, Co), consistent with pK_{a2} reflecting ionization of the metal−water complex.[11] Product affinity measurements suggest that the pK_a values of Glu78 and His265 (in *Ec* LpxC) are 6.5 ± 0.1 and 7.4 ± 0.1, respectively.[19] Furthermore, the pH dependence of NMR chemical shifts (imidazole, $^1H/^{13}C$ HSQC) demonstrated that the pK_a value of the His265 residue is 7.6 ± 0.1 at 50 °C in a mutant of *Aa* LpxC (the peaks in the NMR spectrum were not resolved enough to make the determination in WT LpxC; therefore, a variant containing seven mutations, including H200Y, was used for these experiments).[12] These measurements suggest that the pK_a of His265 is lower than the value of pK_{a2} observed in the pH−rate profile.

To further examine the role of the catalytic zinc ion in the LpxC-catalyzed reaction, we have undertaken a ^{67}Zn solid-state NMR investigation to probe the pH dependence of LpxC as seen by the metal ion. These experiments measure the quadrupole coupling constant (C_q), which is directly related to the electric field gradient tensor.[20] The value of C_q at the nuclide of interest is given by

$$C_q = q_{zz}\left[\frac{e^2}{a_0^3 h}\right]Q \tag{1a}$$

$$= q_{zz} \times 35.24474 \text{ MHz } (\text{for } ^{67}\text{Zn}) \tag{1b}$$

Here Q is the quadrupole moment of the nucleus in question and q_{zz} is defined as the largest absolute value of the computed field gradient tensor in the principal axis system (PAS) described by the diagonalized field gradient tensor q. The traceless field gradient tensor[20] in its PAS frame can be described in terms of q_{zz} and its asymmetry parameter (η_q):

$$|q_{zz}| \geq |q_{yy}| \geq |q_{xx}| \quad \eta_q \equiv \frac{q_{xx} - q_{yy}}{q_{zz}} \tag{3}$$

The units for q_{zz} are atomic units, and the factor of 35.24474 MHz can be computed if the atomic constants (e, a_0, and h) are expressed in cgs units and the value of Q is given as 0.15×10^{-24} cm^2.[21] As one might intuit, the field gradient tensor is sensitive to the local charge around the center of interest. Consider an isolated Zn^{2+} ion that is tetrahedrally coordinated by water ligands. The field gradient at the Zn^{2+} ion (a center of T_d symmetry) would be zero. However, remove one of the protons to make one of the waters a hydroxide, and the field gradient would increase dramatically with the change of a neutral ligand to a charged one. If on the other hand, rather than deprotonating a water ligand, a hydrogen bond acceptor was introduced to one of the water ligands, the electric field gradient would again be nonzero, but it would clearly be a smaller change relative to the change observed from water to hydroxide. Local environmental changes such as these can be probed using the NMR spectroscopy of a quadrupolar nuclide such as Zn^{2+}. These local environmental changes, as well as structural changes such as a carboxylate toggling between uni- and bidentate interactions, can then be modeled utilizing a combined quantum mechanical/molecular mechanical (QM/MM) approach[22−26] to

(16) We utilize the convention of residue numbering from *E. coli* for the *A. aeolicus* enzyme.

(17) Hernick, M.; Fierke, C. A. *Arch. Biochem. Biophys.* **2005**, *433*, 71–84.
(18) McClerren, A. L.; Zhou, P.; Guan, Z.; Raetz, C. R. H.; Rudolph, J. *Biochemistry* **2005**, *44*, 1106–1113.
(19) Hernick, M.; Fierke, C. A. *Biochemistry* **2006**, *45*, 15240–15248.
(20) Cohen, M. H.; Reif, M. G. *Solid State Phys.* **1957**, 5.
(21) Pyykko, P. *Mol. Phys.* **2001**, *99*, 1617–1629.
(22) Gao, J. L.; Truhlar, D. G. *Annu. Rev. Phys. Chem.* **2002**, *53*, 467–505.
(23) Shurki, A.; Warshel, A. *Protein Simul.* **2003**, *66*, 249–313.
(24) Warshel, A. *Annu. Rev. Biophys. Biomol. Struct.* **2003**, *32*, 425–443.
(25) Friesner, R. A.; Guallar, V. *Annu. Rev. Phys. Chem.* **2005**, *56*, 389–427.
(26) Valiev, M.; Yang, J.; Adams, J. A.; Taylor, S. S.; Weare, J. H. *J. Phys. Chem. B* **2007**, *111*, 13455–13464.

predict the electric field gradient tensor and therefore C_q.[27] Herein we present the results of our solid-state NMR experiments on both WT *Aa* LpxC WT and the H265A mutant, as well as the resulting QM/MM modeling of these data.

Experimental Section

Preparation of LpxC. *A. aeolicus* LpxC variants (WT, H265A)[11] in a pET21a vector were overexpressed in *E. coli* (BL21 (DE3) pLysS cells) and purified according to published procedures using DEAE-Sepharose and Reactive Red 120 affinity dye columns at room temperature.[1,4,28,29] The apo-enzymes were prepared by incubation of LpxC (100 μM) with 20 mM dipicolinic acid, 50 μM ethylenediamine tetraacetic acid, 10 mM HEPES, pH 7.5, at room temperature for 1 h.[1,11] Excess chelating agents were removed by washing with buffer using an Amicon Ultra-15 centrifugal filter unit from Millipore (25 mM HEPES, 1.5 mM TCEP, pH 7.5) and passage through PD-10 desalting columns to yield apo-LpxC (1.2−1.8 mM; 25 mM HEPES, 1.5 mM TCEP, pH 7.5). The concentration of the remaining bound metal ions was determined by ICP-MS (0.02−0.04 Fe/LpxC, 0.01−0.11 Zn/LpxC) at the Department of Geology, University of Michigan, by Dr. Ted Huston. For the high-pH samples, the buffer was exchanged by diluting 1 mL of apo-LpxC with 14 mL of 25 mM bis-tris propane, 1.5 mM TCEP, pH 8.7, and concentrating the samples using Amicon Ultra-15 centrifugal filter units (repeat for a total of three washes). The low-pH samples exhibited marked precipitation at high concentrations and therefore could not be prepared in a similar manner. For these samples, the apo-LpxC was diluted 10-fold, dialyzed against 4 L of 25 mM bis-tris, 1.5 mM TCEP, pH 6.2, at room temperature for 1 h, transferred into metal-free conical tubes, frozen, and lyophilized. Lyophilization does not alter catalytic activity (data not shown). Before use, the samples were lyophilized and reconstituted with stoichiometric ^{67}Zn. Dry LpxC (50−80 mg) was reconstituted by adding an equimolar amount of 100 mM ^{67}Zn acetate and resuspended in 150 μL of 30% glycerol/water solution by repeated brief centrifugation and mixing until the solution appeared clear. Each sample was doped with 20 mg of dry cobalt-substituted human carbonic anhydrase isozyme II (Co-hCAII), the pH at ice temperature was adjusted to 6.3 and 8.7 for low and high pH, respectively, using 100 mM NaOH and 100 mM H_2SO_4, and the samples were transferred to 5 mm NMR tubes (cut to a length of 20 mm) and frozen over liquid nitrogen. The ^{67}Zn acetate and Co-hCAII were prepared as previously described.[30]

Solid-State ^{67}Zn NMR. All zinc chemical shifts are referenced with respect to 1 M $Zn(NO_3)_2$(aq) (measured at ambient temperature). The ^{67}Zn spectra were acquired at 10 K utilizing a Varian Unity^{plus} spectrometer with a wide-bore Oxford Instruments magnet operating at 11.7 T (500 MHz for ^{1}H and 31.297 MHz for ^{67}Zn) and a Varian Unity^{Inova} spectrometer with a medium-bore (63 mm) Oxford Instruments magnet operating at 18.8 T (800 MHz for ^{1}H and 50.048 MHz for ^{67}Zn). To obtain cryogenic temperatures (10 K) in the magnets, an Oxford Instruments continuous-flow cryostat was utilized. The cryostat is top-loaded into the bore of the magnet, and a home-built NMR probe is then inserted into the sample space of the cryostat.[31,32] The pulse sequence used was a combination of cross-polarization (CP)[33] with signal detection using the quadrupole Carr−Purcell−Meiboom−Gill (QCPMG) sequence.[34,35] The ^{1}H RF field strength used for CP was 40 kHz with CW decoupling at 62.5 kHz, and the echo train utilized 11.111 kHz ^{67}Zn RF corresponding to selective 15 μs π pulses. Due to the width of the lineshapes we could not acquire them in a single experiment, so the ^{67}Zn offset frequency was stepped every 10 kHz, and then all of the offsets were combined in a sky projection to construct the final spectrum.[36]

The spectra were analyzed using the SIMPSON program.[37] Simulations of the NMR spectra were performed on a Beowulf cluster (composed of 24-Racksaver[38] dual Pentium IV 2.4 GHz Xeon nodes, 40-Verari dual socket, dual core Intel 5140 2.33 GHz Xeon nodes, and 16-Verari dual socket, dual quad Intel 5345 2.33 GHz Xeon nodes) running the Rocks clustering software and utilizing a gigabit Ethernet connection. The final combined stepped frequency experiments were simulated with ideal pulses only.

Ab Initio Molecular Orbital Calculations. Geometry optimizations and calculations of the electric field gradient (EFG) tensors were performed using the QM/MM module[26] of NorthWestChem (NWChem) developed at the Pacific Northwest National Laboratory (PNNL).[39] The structure with accession code 1P42[9] from the Protein Data Bank (PDB) served as a starting point for geometry optimizations. Density functional theory (DFT) was used for the quantum atoms with the exchange-correlation functional defined as the local spin density approximation (LSDA or LDA) utilizing Slater's local spin density exchange[40] and the Vosko, Wilk, and Nusair (VWN) V local spin density correlation functional[41] with an Ahlrich double-ζ basis set with polarization (pAVDZ).[42] The optimization procedure iteratively cycles through the quantum region, the classical solute, and finally the solvent region until the total energy converges to within 10^{-4} hartree. Subsequent property calculations utilized an Ahlrich triple-ζ basis set including polarization functions (pATZV).[43] The Ahlrich basis sets have provided excellent results from prior investigations, hence their use in the present study.[44,45] The QM/MM cutoff utilized in all calculations was 15 Å. A test of our sensitivity to this is shown in the Supporting Information where the effect was negligible for both C_q and η. The calculations were carried out on the following systems: the Beowulf cluster mentioned above or the 11.8 TFlop Hewlett-Packard system (980 dual Intel 1.5 GHz Itanium-2 processors) present in the Environmental Molecular Sciences Laboratory (EMSL) running a version of Linux based on a Red Hat Linux Advanced Server with a QSNet^{II}/Elan-4 interconnect from Quadrics.

Results and Discussion

To reiterate what we know about the pH dependence of k_{cat}/K_M for *Aa* LpxC, there are two ionizations observed in the WT enzyme with pK_a values of 5.8 and 7.9 at 60 °C. The enzyme containing the single mutation H265A also exhibits a bell-shaped

(27) Lipton, A. S.; et al. *J. Am. Chem. Soc.*, in press.
(28) Young, K.; Silver, L. L.; Bramhill, D.; Cameron, P.; Eveland, S. S.; Raetz, C. R. H.; Hyland, S. A.; Anderson, M. S. *J. Biol. Chem.* **1995**, *270*, 30384–30391.
(29) McClure, C. P.; Rusche, K. M.; Peariso, K.; Jackman, J. E.; Fierke, C. A.; Penner-Hahn, J. E. *J. Inorg. Biochem.* **2003**, *94*, 78–85.
(30) Lipton, A. S.; Heck, R. W.; Ellis, P. D. *J. Am. Chem. Soc.* **2004**, *126*, 4735–4739.
(31) Lipton, A. S.; Sears, J. A.; Ellis, P. D. *J. Magn. Reson.* **2001**, *151*, 48–59.
(32) Lipton, A. S.; Heck, R. W.; Sears, J. A.; Ellis, P. D. *J. Magn. Reson.* **2004**, *168*, 66–74.
(33) Pines, A.; Gibby, M. G.; Waugh, J. S. *J. Chem. Phys.* **1972**, *56*, 1776.
(34) Larsen, F. H.; Jakobsen, H. J.; Ellis, P. D.; Nielsen, N. C. *J. Phys. Chem. A* **1997**, *101*, 8597–8606.
(35) Larsen, F. H.; Lipton, A. S.; Jakobsen, H. J.; Nielsen, N. C.; Ellis, P. D. *J. Am. Chem. Soc.* **1999**, *121*, 3783–3784.
(36) Lipton, A. S.; Wright, T. A.; Bowman, M. K.; Reger, D. L.; Ellis, P. D. *J. Am. Chem. Soc.* **2002**, *124*, 5850–5860.
(37) Bak, M.; Rasmussen, J. T.; Nielsen, N. C. *J. Magn. Reson.* **2000**, *147*, 296–330.
(38) Racksaver is now Verari Systems.
(39) Bylaska, E. J.; et al. NWChem, v5.0 ed., Richland, WA 99352, 2006.
(40) Slater, J. C. *The Self-Consistent Field for Molecules and Solids*; McGraw-Hill: New York, 1974; Vol. 4.
(41) Vosko, S. H.; Wilk, L.; Nusair, M. *Can. J. Phys.* **1980**, *58*, 1200–1211.
(42) Schafer, A.; Horn, H.; Ahlrichs, R. *J. Chem. Phys.* **1992**, *97*, 2571–2577.
(43) Schafer, A.; Huber, C.; Ahlrichs, R. *J. Chem. Phys.* **1994**, *100*, 5829–5835.
(44) Lipton, A. S.; Bergquist, C.; Parkin, G.; Ellis, P. D. *J. Am. Chem. Soc.* **2003**, *125*, 3768–72.
(45) Lipton, A. S.; Ellis, P. D. *J. Am. Chem. Soc.* **2007**, *129*, 9192–9200.

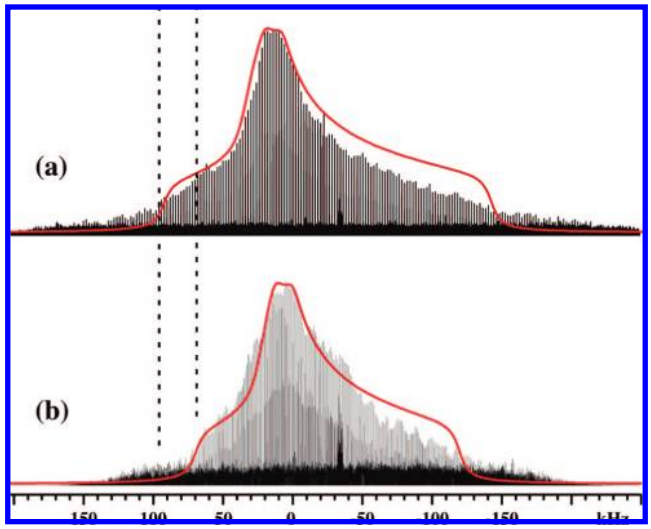

Figure 1. ^{67}Zn NMR data collected at 18.8 T/10 K for WT LpxC prepared at (a) pH 8.7 and (b) pH 6 where each 10 kHz block had a recycle delay of 1 min for 256 accumulations. Simulations using the parameters from Table 1 are in red and overlaid on the respective experimental data.

pH dependence with a pair of ionizations with slightly higher pK_a values.[11] In the double mutant E78A/H265A LpxC only a single ionization is observed (pK_a = 8.4).[11] The question we are attempting to answer is the following: Can we identify which residue(s) are being ionized and which pK_a, if any, reflects the zinc-bound water? To make this determination, we have examined the ionization of WT *Aa* LpxC at various pH values using ^{67}Zn NMR spectroscopy to investigate whether any ionizations are located close enough to the catalytic zinc ion to be reflected in the electric field gradient of this metal ion. The data collected on these samples at 18.8 T are depicted in Figure 1. One can see even from a cursory visual inspection of the experimental data that the spectra vary for samples prepared at different pH values. The spectrum of the high-pH (adjusted to 8.7 at 0 °C) sample (Figure 1a) appears dominated by a lineshape with a C_q of 14.2 MHz[46] with perhaps ≤20% of a second species (not included in the simulated lineshape). Utilizing 30% as an upper limit and 10% as the low end of the amount of the minor component, we can estimate that the apparent pK_a value for this ionization is between 8.2 and 7.8. This may be an underestimation of the value of the pK_a as changes in the pH caused by lowering the temperature are not included; the buffer utilized for the high-pH sample may allow the sample pH to increase by as much as 1.5 units upon cooling,[47] which shifts the measured pK_a range by a similar amount and needs to be accounted for in a pK_a determination. The sample at pH 6.3 (adjusted at 0 °C) (Figure 1b) shows what appears to be two lineshapes with the C_q of the dominant species at 12.9 MHz (possibly the minor species at high pH) and an asymmetry parameter (η_q) of 0.90, and the second minor species contributing approximately 25% of the observed lineshape with a C_q near 10 MHz (not included in the simulated spectrum of Figure 1b). We propose that these two lineshapes represent two different ionization states of LpxC at pH 6.3 with a pK_a value that is between 6.0 and 5.5, assuming a 10% error in the relative concentrations. This pK_a does not account for any change in pH that may have occurred on cooling to cryogenic temperatures, and an effort to determine the pH at cryogenic temperatures for each of the buffers utilized is under way. While the major species manifest about a 10% difference in C_q, the results clearly show an ionization that we ascribe to pK_{a1}. The data deviate from the ideal lineshapes shown in Figure 1 due to a combination of slight structural disorder (these are not crystalline powders) and possibly an orientational dependence of the CP conditions, resulting in a loss of efficiency toward the end of the spectra. A further analysis of the low-pH data is supplied in the Supporting Information.

The ionization observed at high pH may reflect either the zinc-bound water or one of the nearby active site side chains. Since the estimated pK_a value in these experiments approaches the reported pK_a value of His265, and its side chain is located within 3−3.5 Å of the zinc−water complex, it is possible that the ionization observed in these experiments reflects that of His265. To test this hypothesis, we repeated the ^{67}Zn NMR experiments on the H265A mutant at both pH 6.3 and pH 8.7. The spectra collected at a magnetic field strength of 18.8 T are shown in Figure 2 with simulated lineshapes calculated using identical parameters where C_q is 9.55 MHz and η_q is 0.87. The signal outside of the region from +60 to −100 kHz originates

Table 1. Quadrupole Coupling Information from Experiment and Theory

	C_q(MHz)	η_q	δ_{iso}[a] (ppm)
WT, pH 6, site 1	12.9	0.90	133
WT, pH 6, site 2	∼10	?[b]	170
WT, pH 9	14.3	0.92	284
model 1a	−13.4	0.48	−[c]
model 1b	15.6	0.95	−
model 1c	18.7	0.65	−
model 2a	17.4	0.56	−
model 2b	−22.7	0.98	−
model 2c	−24.7	0.79	−

[a] Isotropic chemical shift relative to the peak for 1 M $Zn(NO_3)_2$(aq) at ambient temperature. [b] The asymmetry parameter could not reliably be extracted from the data; see the Supporting Information. [c] The isotropic chemical shifts were not calculated for the QM/MM models.

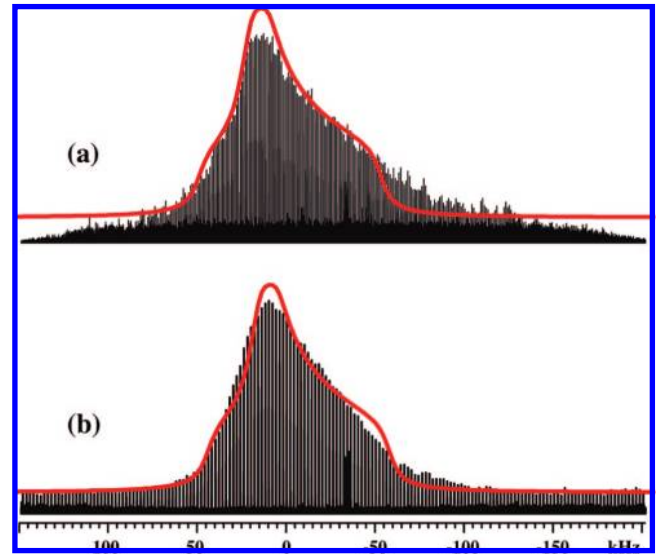

Figure 2. ^{67}Zn NMR data collected at 18.8 T/10 K for H265A LpxC prepared at (a) pH 8.7 and (b) pH 6 where each 10 kHz block had 512 accumulations with recycle delays of 30 and 60 s, respectively. Identical simulations (in red) using a C_q of 9.55 MHz and an η_q of 0.87 are overlaid on both data sets.

(46) Note that the NMR experiment can only extract an absolute value of C_q and the sign is not determined.
(47) Sieracki, N. A.; Hwang, H. J.; Lee, M. K.; Garner, D. K.; Lu, Y. *Chem. Commun.* **2008**, 823–825.

from the outer transitions and not the $\langle \pm 1/2 \rangle$ transition,[32] which is of interest here. There are two important observations one can make from this experiment. First, the value of C_q at the Zn^{2+} ion is sensitive to the presence or absence of His265, as the value of C_q is reduced by either 3.3 or 5.6 MHz (depending on the pH) relative to that of the WT LpxC. Second, the data show only subtle differences between the two pH values, in particular the region from −40 to −100 kHz (this is highlighted further in the Supporting Information). Therefore, the ionization at high pH observed in the k_{cat}/K_M pH−rate profile of the H265A mutant must reflect ionization of a group that is located far enough away from the zinc ion such that it has only a minor effect on the electric field gradient of the metal ion. Furthermore, these data imply that the ionization observed for the WT enzyme at high pH in these NMR experiments reflects either His265 or a group located in close proximity to both His265 and the zinc−water complex. This finding suggests that the apparent pK_a of His265 (or a group linked to His265) in WT LpxC is between pH 7.8 and pH 8.2 (with an estimated temperature correction of at least 1.5 pH units the pK_a at 10 K appears to be ≥9.5), slightly higher than previous reports at higher temperatures. A remaining question then is whether the ligand bound to the zinc ion under these conditions is water or hydroxide.

To identify the nature of the fourth ligand coordinated by the catalytic metal ion, we have performed several QM/MM calculations on the active site of LpxC to predict the C_q of each model. The following deletions from the X-ray structure (PDB code 1P42) were made prior to our modeling: the entire B chain, six additional bound zinc atoms (as we only added 1 equiv of zinc instead of the large excess used in this structure), and the myristic acid ligand. Beginning with the catalytic metal ion, we include as quantum the side chains of His79, Asp242, and His238 and a water molecule. Also included are the hydrogen-bonding partners to these ligands, namely, a water for $N_\varepsilon H$ of His79, a water for $O_{\delta 2}$ of Asp242, and the backbone CO of Ala189 for $N_\varepsilon H$ of His238. The GABC residues in question, Glu78 and His265, are also represented as quantum with their respective hydrogen-bonding partners. The starting active site, prior to optimization, is depicted in Figure 3. Also shown in this figure are the water molecules identified in the crystallography that we refer to as the "water network", as well as Asp246 and Asn268 (located behind His265), for their potential to interact with His265, each other, and the water network of the active site. Unless otherwise indicated, the glutamate and aspartate residues are included as nonprotonated carboxylates, COO^-.

We first examined the likely candidates responsible for the high-pH ionization observed in the NMR spectra, namely, His265 and the zinc-bound water. To test these possibilities, we generated six models, including the three possible protonation states of the imidazole ring of His265 ($N_\varepsilon H$, HIE; $N_\delta H$, HID; charged diprotonated imidazole ring, HIP) with either water or hydroxide coordinated to the zinc. The optimized geometries are depicted in Figures 4 and 5, where Figure 4 (models 1a−c) has water bound to zinc and the analogous models in Figure 5 have hydroxide bound to the metal (models 2a−c). The predicted C_q values are contrasted with the experimentally derived values in Table 1. These models were also tested utilizing other functionals (B3LYP, PBE, and RHF) with similar resulting trends (however, RHF and B3LYP consistently overestimate C_q) that are tabulated in the Supporting Information. From this comparison we can rule out some of the proposed models as the predicted C_q values are out of range

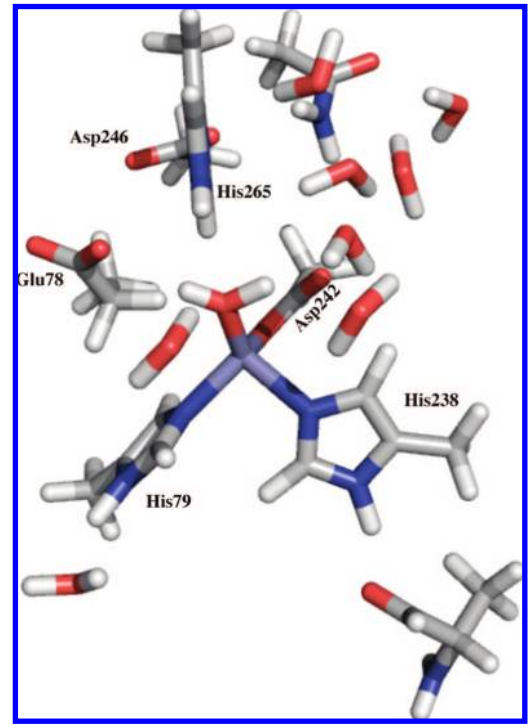

Figure 3. Representation of the starting quantum region for the QM/MM calculations generated with MacPyMol 1.0r2 from PDB structure 1P42.

of the experimental values. Both monoprotonated forms of His265 with hydroxide bound to the zinc predict C_q values that are too large (recall that we are comparing the absolute values as the sign is not determined by the NMR experiment). If we allow for only a 1−2 MHz error in our predictions, then we can likewise rule out models 1c and 2a. This leaves models 1a and 1b as the only proposed models consistent with our data. We also explored the possibility of the five-coordinate species proposed by Gennadios et al.[48] through a QM/MM model. However, we find that this species is not quantum mechanically stable and the second water ligand quickly dissociates from the zinc upon geometry optimization.

The two remaining models represent ionization of His265 with water bound to the zinc. The predicted change in C_q upon ionization is on the order of 2 MHz, which agrees qualitatively with the small increase observed upon going from the low-pH to high-pH samples. Therefore, the calculations indicate that the high-pH ionization observed in the ^{67}Zn NMR spectrum reflects deprotonation of His265 and that ionization of zinc-bound water does not occur over this pH range. In these models, the low-pH form has His265 doubly protonated; one imidazole NH (δ) forms a hydrogen bond with the carboxylate of Asp246, while the other NH (ε) forms a hydrogen bond with the carboxylate of Glu78. This same Glu78 oxygen also hydrogen bonds with the zinc-bound water. The second proton of this zinc-bound water molecule is connected to the carboxylate of Asp242 through a single intervening water. This intervening water is also hydrogen bonded to the rest of the water network, which is composed of hydrogen bond linkages from Asn268 down to Asp242 and then around the metal-bound water to Glu78. The waters in this network are depicted in ball and stick representation including the zinc-bound water/hydroxide. In the

(48) Gennadios, H. A.; Whittington, D. A.; Li, X.; Fierke, C. A.; Christianson, D. W. *Biochemistry* **2006**, *45*, 7940–8.

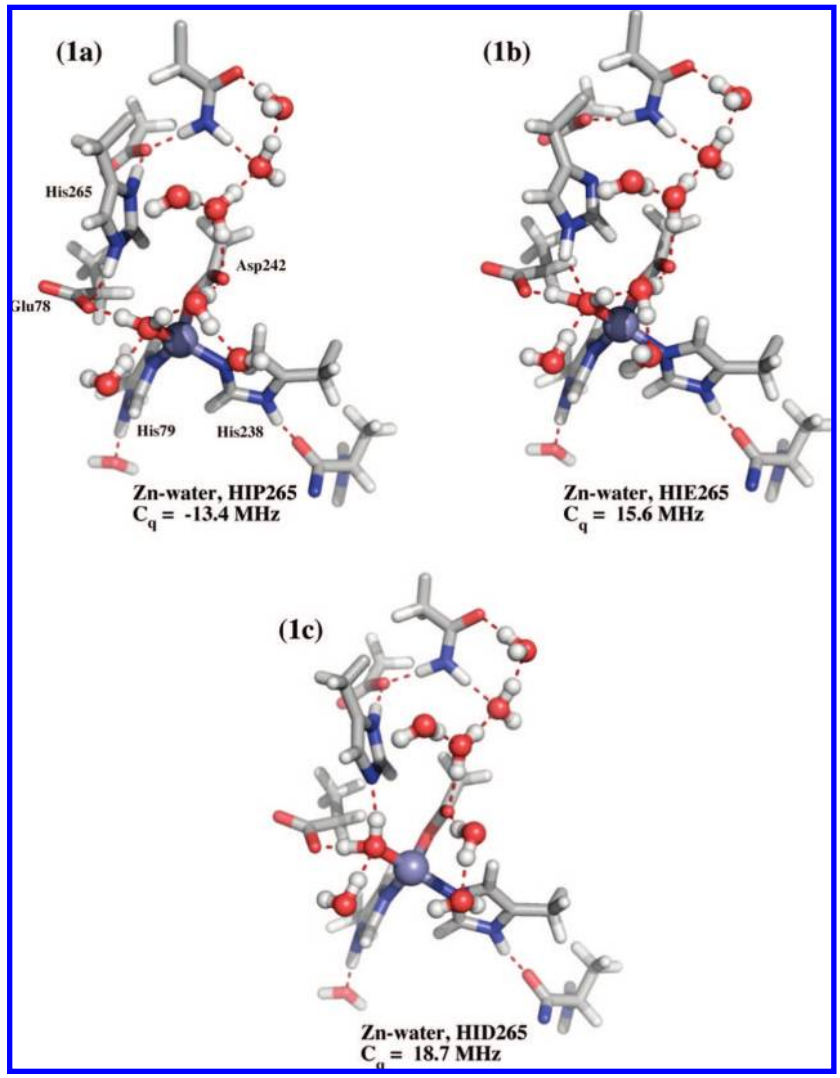

Figure 4. QM/MM-optimized quantum regions of WT LpxC with water bound to the zinc and His265 protonated as (1a) doubly protonated (HIP), (1b) singly protonated at N_ε (HIE), and (1c) singly protonated at N_δ (HID). The water network, including zinc-bound water, is represented as balls and sticks, and hydrogen bonds within 2.0 Å are drawn as red dashed lines.

figures, a hydrogen bond is shown as a red dashed line using a cutoff of 2.0 Å.

Focusing on models 1a and 1b, the deprotonation of $N_\delta H$ (model 1b) results in only minor structural changes. The main difference in these models is the orientation of His265. In the doubly protonated form (model 1a) this side chain is turned such that the ε proton of the imidazole ring hydrogen bonds with Glu78 $O_{\varepsilon 1}$; however, in model 1b it reorients such that the ε proton hydrogen bonds to the oxygen of the zinc-bound water. This does not appreciably change the Zn−O distance, but there are small distance changes observed involving His79 and His238. In model 1a, both histidines have hydrogen-bonding partners that are within 1.5 Å, but for model 1b, the CO of Ala189 moves out slightly from 1.5 to 1.6 Å and the water hydrogen bonding to His79 moves out from 1.4 to 1.5 Å. Additionally, the Zn−N bond of His79 is extended 1/10 Å to 2.0 Å. These changes modulate the electric field gradient at the metal ion to maintain a constant charge. Nonetheless, these changes are detectable in the ^{67}Zn NMR spectra. Furthermore, the coupling of His265 to the metal-bound water could account for a dependence of this pK_a on the identity of the metal ion.[11]

We have also performed QM/MM calculations on models of the active site of the H256A mutant with both water and hydroxide bound to the zinc. The optimized quantum regions are shown in Figure 6 along with the predicted C_q values. The hydroxide form again predicts an electric field gradient that is too large by almost a factor of 2.5 than that observed in our experiment. The water form predicts a value (C_q of 14.7 MHz) that is still too large, but closer to our experimental result (C_q of 9.55 MHz). This is consistent with our previous calculations on the WT system and leads us to suggest that the zinc-bound water does not ionize in the resting H265A mutant under the range of pH values examined here. A note about the model with water bound to the Zn^{2+} ion is that a proton of the metal−water complex is transferred to Glu78 via a solvent water (the resulting structure is shown in Figure 6c). This could account for the predicted value of C_q being overestimated.

The final series of calculations were performed to probe the possibility of an ionization of Glu78 as a source of the pK_a observed at low pH in the ^{67}Zn NMR spectra of both wild-type and H265A LpxC. Mutagenesis studies have previously suggested that ionization of Glu78 leads to a decrease in catalytic

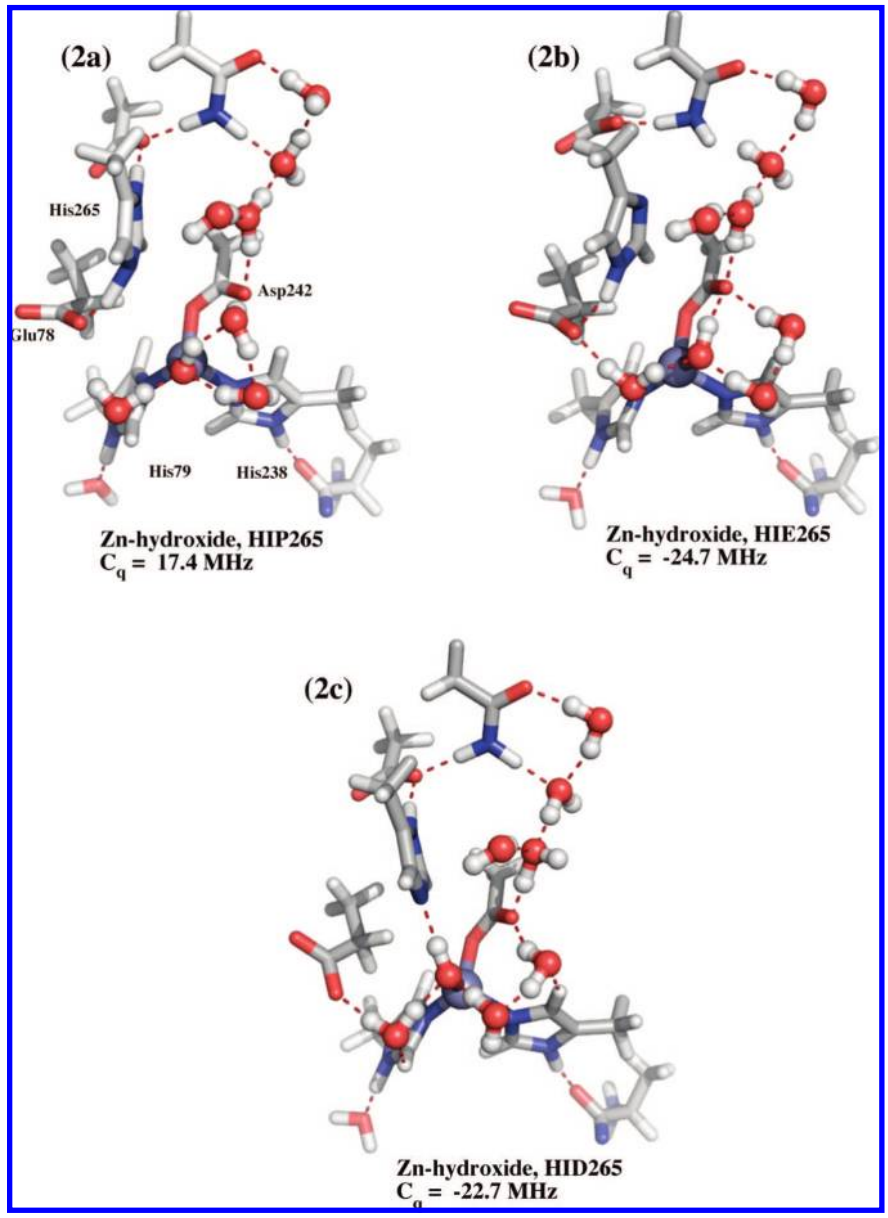

Figure 5. QM/MM-optimized quantum regions of WT LpxC with hydroxide bound to the zinc and His265 protonated as (2a) doubly protonated (HIP), (2b) singly protonated at N_ε (HIE), and (2c) singly protonated at N_δ (HID). The water network, including zinc-bound OH, is represented as balls and sticks, and hydrogen bonds within 2.0 Å are drawn as red dashed lines.

activity at low pH in both enzymes.[11,18] We began by making the assumption that His265 is in a doubly protonated state at pH 6.3 (recall that our data indicate that the higher pK_a in the NMR spectrum reflects ionization of His265 for the WT enzyme). There are two possible O_ε atoms in a Glu side chain that could be protonated, so we optimized the geometries starting from both states. These same calculations were also performed on the H265A mutant. The optimized geometries are depicted in Figure 7, and the predicted C_q values of these models are summarized in Table 2. It is interesting that for the WT enzyme there is an impact on the predicted field gradient of the zinc depending upon which O_ε is protonated. Protonating $O_{\varepsilon 1}$ (closest to the zinc and His265) leads to a predicted value of C_q that is between the experimentally determined values for the two species observed at low pH and lower than the value calculated for model 1a. However, protonation of $O_{\varepsilon 2}$ leads to a calculated value (C_q of −13.0 MHz) similar to that of model 1a (C_q of −13.4 MHz), which makes them difficult to distinguish experimentally.

The values of C_q calculated for the H265A LpxC mutant with Glu78 protonated in either position (C_q of 7.6 MHz) are now more in agreement with the experimentally determined value of C_q (C_q of 9.55 MHz, within a 2 MHz error limit). That these calculations predict similar values of C_q is presumably due to the absence of an interaction with His265. These data suggest that in the H265A mutant Glu78 is protonated over the range of pH values investigated (6.3−8.7). The catalytic mechanism of the H265A mutant is currently unclear. The loss of His265 presumably forces the reaction to proceed via a different mechanism, albeit with decreased efficiency (as demonstrated by the overall decrease in activity for the Ala mutants). One possibility is that Glu78 functions as both the general acid and the general base. However, the high pK_a for E78 proposed from the calculations is difficult to reconcile with the observed pH

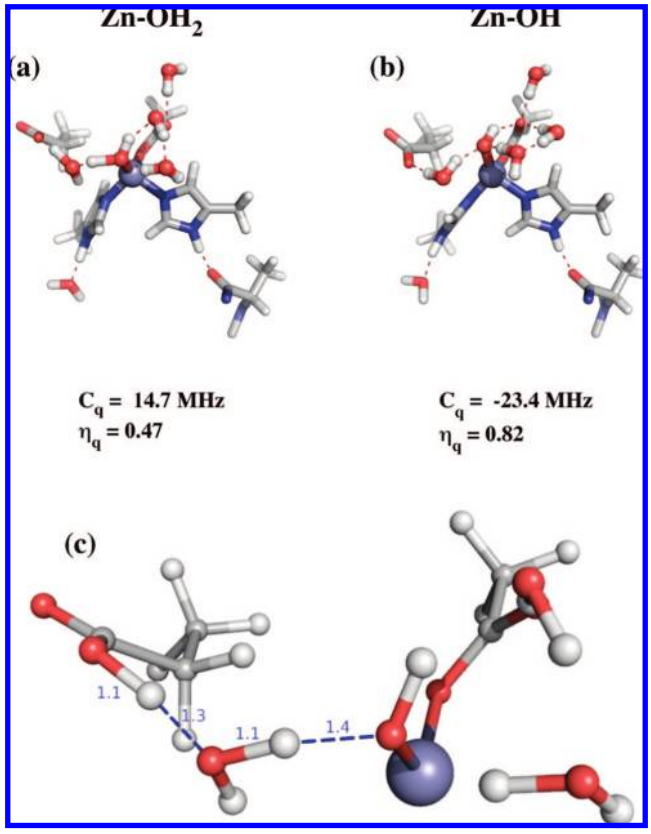

Figure 6. QM/MM-optimized quantum regions of H265A LpxC with (a) water bound to the zinc ion and (b) hydroxide coordinated to the metal ion with the respective predicted quadrupole coupling parameters. Shown in (c) is an expansion of (a) showing the result of a proton transfer of the zinc−water complex to a solvent water which protonates Glu78.

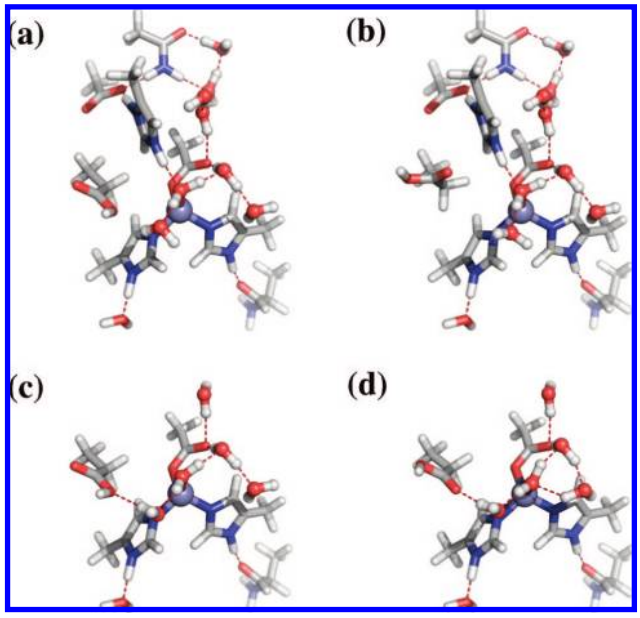

Figure 7. QM/MM-optimized quantum regions of WT LpxC with doubly protonated His265, water bound to zinc, and a proton added to (a) Glu78 $O_{\varepsilon 1}$ and (b) Glu78 $O_{\varepsilon 2}$ and H265A LpxC with water bound to zinc and (c) Glu78 $O_{\varepsilon 1}$H and (d) Glu78 $O_{\varepsilon 2}$H.

dependence of k_{cat}/K_M for this mutant (6.0 and 8.2)[11] unless the rate-limiting step in this reaction is protonation of the leaving group. Another possible catalytic mechanism for the mutant is that an alternative group, such as Asp246 or Asp242, functions as a general base with a pK_a near 6, while Glu78 functions as a general acid with a high pK_a. A third alternative is that the reactive form of the enzyme has a zinc−hydroxide complex and protonated Glu78, as illustrated in Figure 6c.

Table 2. Predicted ^{67}Zn Electric Field Gradient of LpxC with a Protonated Glu78

model	V_{zz}	C_q (MHz)	η_q
WT Glu78 $O_{\varepsilon 1}$H	−0.320112	−11.28	0.41
WT Glu78 $O_{\varepsilon 2}$H	−0.369776	−13.03	0.29
H265A Glu78 $O_{\varepsilon 1}$H	0.216468	7.63	0.53
H265A Glu78 $O_{\varepsilon 2}$H	0.217273	7.66	0.55

Conclusions

We have shown that, for the resting enzyme, in the absence of substrate, the ^{67}Zn NMR spectrum is sensitive to a change in pH. The ionization that is observed around pH 8.0 (not corrected for the temperature dependence of the buffer) is ascribed to the deprotonation of the side chain of His265. This conclusion is bolstered by the predicted C_q values of models 1a (the diprotonated His265) and 1b (single proton on His265 N_ε). The observed changes in C_q (1.5 MHz) are significantly smaller than what is expected for ionization of a group directly coordinated to the metal (for LpxC we predict a change on the order of 5−7 MHz utilizing the QM/MM modeling). In addition, the QM/MM models suggest that the pK_a for the deprotonation of the zinc-bound water in LpxC is high (>10.2, which is the estimated pH of the "high"-pH sample after it is cooled to cryogenic temperatures). Furthermore, the high-pH ionization disappears in the H265A mutant, and in fact, no ionization at high pH is detectable as reflected in the NMR spectroscopy of the zinc. Therefore, all of the data indicate that the ionization observed in the ^{67}Zn spectrum at high pH is due to deprotonation of His265 in the active site of LpxC. The ionization observed in the NMR spectrum at low pH could be due to deprotonation of Glu78. However, for protonation of the carboxylate $O_{\varepsilon 1}$ the predicted value of C_q (−11.3 MHz) is within the allowable error of the experimental values measured for either the minor component (C_q = 10 MHz) or the dominant form (C_q near 13 MHz) of the enzyme at pH 6. A protonated $O_{\varepsilon 2}$ would most likely be indistinguishable from the nonprotonated Glu78. In the H265A LpxC mutant prepared at low pH, it is difficult to recognize the presence of a minor species given the lack of features of the line shape; nonetheless, the evidence suggests that Glu78 is protonated in this mutant under these conditions, indicating that the reaction proceeds using an alternate mechanism.

In summary, we have examined the ^{67}Zn NMR spectrum of LpxC as a function of pH. We observe two ionizations, neither of which corresponds to zinc-bound water. Rather, the observed ionizations in the ^{67}Zn spectra of wild-type LpxC likely reflect deprotonation of Glu78 at low pH followed by deprotonation of His265 at higher pH. It is tempting to conclude that these same ionizations are observed in the k_{cat}/K_M pH−rate profile. However, the large difference in temperatures makes it difficult to make a direct comparison between the cryogenic NMR data and the kinetic data acquired at ambient or elevated temperatures. Experiments are currently under way to quantify the change in pH of a buffer system due to changes in temperature, which will enable a correlation between data acquired in varying environments. Regardless, the agreement between experiment and theory indicates that over the pH range investigated LpxC maintains water bound to the zinc ion in the active site.

Acknowledgment. This work was supported by grants from the National Institutes of Health (Federal Grants EB-2050 to PNNL and GM40602 to C.A.F.) and the Cystic Fibrosis Foundation (Grant HERNIC05F0 to M.H.). This research was carried out in the EMSL (a national scientific user facility sponsored by the U.S. Department of Energy's (DOE's) Office of Biological and Environmental Research) located at PNNL and operated for the DOE by Battelle. Computations were performed in part using the Molecular Science Computing Facility in the EMSL. NWChem versions 5.0 and 5.1, as developed and distributed by PNNL, P.O. Box 999, Richland, WA 99352, and funded by the U.S. DOE, were used to obtain some of these results.

Supporting Information Available: Complete refs 7 and 39, fit of both species in the NMR spectra (18.8 and 11.7 T) of the low-pH preparation of WT LpxC, a closer examination of the differences in the solid-state NMR data collected for H265A LpxC, a test of the QM/MM cutoff parameter performed on model 1a, and a survey of different DFT functionals (LDA, B3LYP, and PBE are compared with RHF) to test our property calculations. This material is available free of charge via the Internet at http://pubs.acs.org.

JA801776C